

Feature-augmented Trained Models for 6DOF Object Recognition and Camera Calibration

Kripasindhu Sarkar^{1,2}, Alain Pagani¹ and Didier Stricker^{1,2}

¹*German Research Center for Artificial Intelligence (DFKI), Kaiserslautern, Germany*

²*Technical University Kaiserslautern, Kaiserslautern, Germany*

{kripasindhu.sarkar, alain.pagani, didier.stricker}@dfki.de

Keywords: 6DOF Object Recognition, Calibration, Natural Calibration Rigs, Feature-augmented 3D Models.

Abstract: In this paper we address the problem in the offline stage of 3D modelling in feature based object recognition. While the online stage of recognition - feature matching and pose estimation, has been refined several times over the past decade incorporating filters and heuristics for robust and scalable recognition, the offline stage of creating feature based models remained unchanged. In this work we take advantage of the easily available 3D scanners and 3D model databases, and use them as our source of input for 3D CAD models of real objects. We process on the CAD models to produce feature-augmented trained models which can be used by any online recognition stage of object recognition. These trained models can also be directly used as a calibration rig for performing camera calibration from a single image. The evaluation shows that our fully automatically created feature-augmented trained models perform better in terms of recognition recall over the baseline - which is the tedious manual way of creating feature models. When used as a calibration rig, our feature augmented models achieve comparable accuracy with the popular camera-calibration techniques thereby making them an easy and quick way of performing camera calibration.

1 INTRODUCTION

The progress in the field of Structure From Motion (SfM) made it possible to have 3D models reconstructed from unordered images. Since these models are a result of matching features across several images, any 3D point in the reconstructed sparse model can be associated with a variety of view dependent descriptors. This association of 3D points - to - 2D descriptors forms the pillar of most of the feature based detection where the features, extracted from a given input image, are matched to that of the feature augmented 3D models and subsequently, a *6 DOF recognition* is made [Skrypnyk and Lowe, 2004, Hao et al., 2013, Collet Romea et al., 2011, Collet Romea and Srinivasa, 2010, Irschara et al., 2009].

Therefore, we can summarize all the *feature based recognition* methods in the following steps:

1. *Building models (offline training stage)*. In the first step, feature-augmented-3D-models are constructed for each of the objects which is to be recognized. For each of the real objects, a set of images from several directions are taken (usually around 50 - 80 [Collet Romea and Srinivasa, 2010, Collet Romea et al., 2011]), SfM is per-

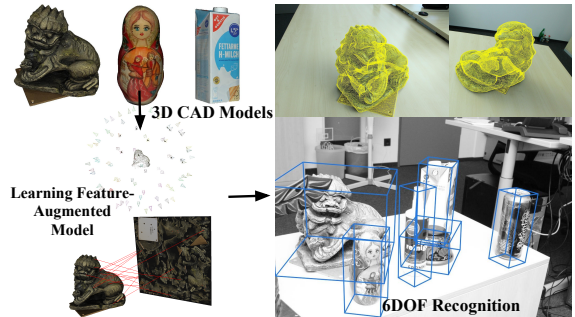


Figure 1: Feature-augmented models for 6DOF object recognition. Starting with 3D CAD models our method produces ‘trained-models’ that can be used by any online recognition framework for 6DOF recognition.

formed, and then finally, view dependent features for each 3D point in the obtained reconstruction are merged using a clustering or averaging technique. In the end of this step we have a set of feature-augmented-3D-models which we will refer here as ‘model’.

2. *Recognition (online stage)*. The online stage involves object recognition in a query image using the models learnt in the offline stage. Image features extracted from the query image are matched

against those in the stored models to get sets of 2D-3D correspondences. Using the correspondences, the pose of the object is found by solving for the projection matrix by one of the dedicated Perspective-n-Points (PnP) methods [Dementhon and Davis, 1995, Lepetit et al., 2009]. This step is usually integrated with outlier removal methods to handle outliers introduced in the matching stage.

There has been several variations of the online stage [Skrypnyk and Lowe, 2004, Collet Romea et al., 2011, Hao et al., 2013] - mostly to make the recognition faster and robust, but the training stage remained more or less unaltered in its original form. The inherent problem in the offline training stage is unaddressed in all the available methods. The problem lies in the amount of manual work involved to create a feature-augmented-3D-model. The main pain-point is to take hundreds of pictures for each model and segment each of them manually before feeding them to SfM. [Hao et al., 2013] used a painted turntable top and a clean background with controlled lighting to reduce the pain of manual capturing, but it still produces lot of outlier model points. Also, producing models on such a controlled environment for object recognition is not scalable to new objects in a new location.

In this paper we address the problem associated with the training stage and propose a method to eliminate all the manual work involved in the existing methods. Here, we accept 3D CAD models to be recognized as input, and produce trained feature-augmented-models as output which can be used by the online stages of any of the recognition methods stated above.

Since the information of 3D to 2D correspondences is already available and encoded in our trained model, we can directly leverage this information to find the intrinsic of the query image. Therefore, we provide a way of directly calibrating an image containing one of the models. Our models trained out of ordinary objects can be just used as a marker for performing calibration without the need of specially designed calibration rigs.

Therefore, our contribution for this paper is a set of algorithms and methods which operates on 3D CAD models to produce feature augmented models for 6DOF recognition and calibration. Because of the capability of the trained models for performing recognition with full pose, our method is very practical for robotic manipulations of objects (such as grasping or other interactions) starting from a single 2D image frame.

It might appear that acquiring CAD models for itself can be a tedious task. But, this is not true in the present situation where cheap and accurate 3D scan-

ners are available in most Robotics and Vision labs. This is because of the boost in a separate branch of research in the topic of 3D computer vision and object recognition/registration in 3D point clouds. In many of these methods, CAD models remain the source of input for processing and extracting different features or other information which are used with that of the scene point-cloud for solving a particular problem (eg. 3D recognition) [Tombari et al., 2010, Rusu et al., 2010, Aldoma et al., 2012]. We do a similar task and process on CAD models to extract information. But instead of point cloud, we perform a full 6DOF recognition in a simple 2D image using the processed data. Our approach can be viewed as the combination of techniques from 2D and 3D computer vision.

In addition to the large variety of easily available 3D scanning hardwares [D'Apuzzo, 2006], we also have now simple software solutions for 3D acquisition where CAD models can be acquired using off-the-shelf hardware. The scanner we used in our experimentation, 3Digify [3Digify, 2015], is one such example where any two household cameras and a projector can be used with the software to make a powerful 3D scanner.

Our methods use two ways to generate 3D points - 2D features correspondences. The first approach is a simple method that uses the texture maps associated with the 3D models to get the 2D feature information for 3D points. The second approach is more closer to the traditional method that takes virtual snapshots of the 3D model from several directions based on a snapshot model and subsequently matching features among the snapshots to rebuilt a feature-augmented model. Our methods along with the recognition pipeline is summarized in Figure 1. The details of the methods are provided in the Section 3.

2 RELATED WORK

Object recognition is one of the key topic in Computer Vision involving several techniques. In this section we will limit our focus to 6DOF object recognition methods which uses 2D local features. This has been a very popular topic which started with the invention of the robust local feature descriptors - SIFT [Lowe, 2004]. The first application of these descriptors towards pose detection in a scene, used them to compute multi-view matches and perform structure from motion to generate feature-augmented scene model. This learned model was then used for scene recognition with full pose estimation [Skrypnyk and Lowe, 2004].

The most robust recognition application in this principle is MOPED [Collet Romeo et al., 2011] where the authors perform the online recognition stage efficiently by clustering the features in the image space before searching for an object, removing many outliers in this process before the matching step. Their training stage still uses the same technique of taking multiple images (around 50) of objects from different directions, segment them manually and then feed them to their training software. Even with their elegant online recognition technique, adding training models to be recognized still becomes problematic and inconvenient because of the amount of manual work involved in the training stage.

The latest work in this area is [Hao et al., 2013] which once again address the problems in the online stage to make it more scalable and robust. To handle spurious 2D-to-3D correspondence that increases the number of RANSAC iterations, the authors proposed efficient filtering methods in the first place. They applied a local filtering step which efficiently checks every individual correspondence in a local region, based on both statistical and geometric cues including spatial consistency and co-visibility. They further filter the spurious correspondences by a global filtering step which is performed on every correspondence pairs which leverage some finer-grained 3D geometric cues to evaluate the compatibility between every two correspondences. They could, in the end, perform efficient detection on a database of 300 models. Once again, the problems in the training stage is unattended.

3 FEATURE-AUGMENTED MODELS

Our method takes a textured 3D model as an input and produces feature augmented *trained model*. We first provide a simplified notation of a textured 3D model which we will be using in this paper. A textured 3D model $\mathcal{M} = \{\mathcal{V}, \mathcal{T}, \mathcal{F}, I\}$ consists of a set of vertices \mathcal{V} , a set of texture coordinates \mathcal{T} , a set of faces \mathcal{F} and a texture-map image I . Each vertex $v \in \mathcal{V}$ denotes a 3D point having its location information, (x, y, z) . Each texture coordinate $t \in \mathcal{T}$ is a two dimensional coordinate in texture space. Each face $f \in \mathcal{F}$ denotes a face of the 3D model formed by a list of vertices from V and their corresponding texture coordinates. In our case, we consider only triangulated 3D models having only triangular faces ie. $f = \{v_{f1}, v_{f2}, v_{f3}\}$ where $v_{fi} = \{v_i, t_i\}$ and $v_i \in V, t_i \in T$.

Given such a model $\mathcal{M} = \{\mathcal{V}, \mathcal{T}, \mathcal{F}, I\}$, our goal is to produce a feature augmented model or a *trained model* $m = \{V\}$, where $v = (\mathbf{p}, d_m) \in V$ and \mathbf{p} lies on

Algorithm 1: Texture-map based training.

Input: A 3D model $\mathcal{M} = \{\mathcal{V}, \mathcal{T}, \mathcal{F}, I\}$

Output: A trained model $m = \{V\}$

- 1: **Init:** $V \leftarrow \emptyset$
 - 2: Extract image features $\mathfrak{F} = \{(\mathbf{k}_i, d_i)\}$ in I
 - 3: \triangleright where \mathbf{k}_i is the keypoint location in I and d_i is the feature descriptor
 - 4: **for all** features (\mathbf{k}_i, d_i) **do**
 - 5: Find the face $f = \{v_{f1}, v_{f2}, v_{f3}\} \in \mathcal{F}$, $v_{fj} = \{v_j, t_j\} \mid k_i$ lies on and inside (t_1, t_2, t_3)
 - 6: Find barycentric coordinates $(\lambda_1, \lambda_2, \lambda_3)$ of k_i w.r.t. (t_1, t_2, t_3)
 - 7: $\mathbf{p} \leftarrow \lambda_1 \mathbf{v}_1 + \lambda_2 \mathbf{v}_2 + \lambda_3 \mathbf{v}_3$
 - 8: $V \leftarrow V \cup (\mathbf{p}, d_i)$
 - 9: **end for**
 - 10: **return** $m = \{V\}$
-

the surface of m (lies in one of the faces in F). d_m the *model feature*, represents a local feature descriptor encoding the local visual information of p . For the later part of snapshot based training, we relax the requirement of p to lie on the surface of m to the requirement that a similar transformation (a scaled rotation followed by translation) of p should lie on the surface of \mathcal{M} .

3.1 Texture Map Based Training

Texture mapping is a graphic design process in which a two-dimensional (2D) surface, called a texture map, is ‘wrapped around’ a three-dimensional (3D) object. Thus, the 3-D object acquires a surface texture similar to that of the 2-D surface. In a 3D model $\{\mathcal{V}, \mathcal{T}, \mathcal{F}, I\}$, each vertex v_{fi} in a face $f \in \mathcal{F}$ is assigned a texture coordinate $t_i = (u_i, v_i)$ in the texture space (also known as a UV coordinate) along with a 3D point $v_i \in \mathcal{V}$. They are the normalized texture-image pixels in I assigned to the vertices of that face. For a face $f = \{v_{f1}, v_{f2}, v_{f3}\}$ with $v_{fi} = \{v_i, t_i\}$ and $v_i \in \mathcal{V}, t_i \in \mathcal{T}$, the texture pixel assigned to the vertices v_i is $I(t_i) = I(u_i, v_i)$, the image pixel of I at (u_i, v_i) . Textured pixel assigned to a point p lying in the face f but not necessarily in one of the three vertices, is $I(int(t_1, t_2, t_3))$, where $int(a, b, c)$ is a 2D interpolation of the points (a, b, c) with coefficients derived from the relation between p and v_i s.

The most popular and widely used interpolation is the linear interpolation of the textured vertices t_i s, and the interpolation coefficients are derived from the Barycentric coordinate of the point p with respect of the vertices v_i s. For a triangle with vertices v_1, v_2, v_3 , each point p located inside and lying on the triangle can be written as a unique convex combination of three vertices. In other words, there is a

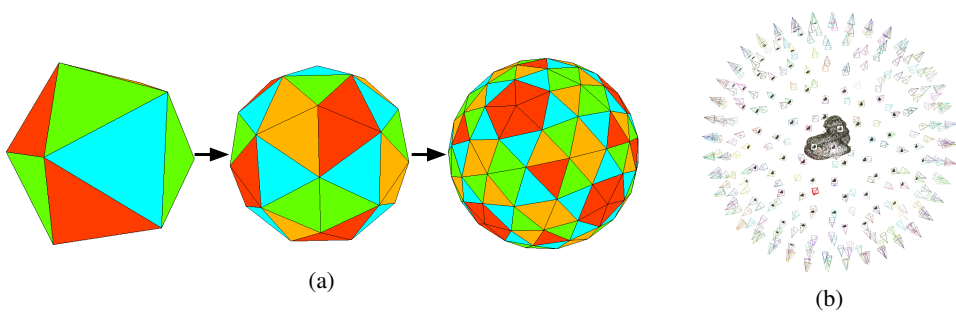


Figure 2: (a) Icosahedron and its recursive subdivision to approximate a sphere for taking snapshots. The camera is positioned at the center of each face and is pointed towards the 3D model kept at the center of the polyhedron. (b) The generated point cloud from the triangulation on the resulted snapshots and the position of the virtual cameras.

unique sequence of three numbers, $\lambda_1, \lambda_2, \lambda_3 \geq 0$ such that $\lambda_1 + \lambda_2 + \lambda_3 = 1$ and $p = \lambda_1 v_1 + \lambda_2 v_2 + \lambda_3 v_3$. $(\lambda_1, \lambda_2, \lambda_3)$ is called the Barycentric coordinates of the point p with respect to the triangle (v_1, v_2, v_3) . With these coefficients for linear interpolation, the textured pixel of any point p lying inside the face with vertices v_1, v_2, v_3 is given by $I(p')$, where $p' = \lambda_1 t_1 + \lambda_2 t_2 + \lambda_3 t_3$ and λ_i are the Barycentric coordinates of p with respect to the vertices v_i .

Note the mapping $p \mapsto p'$, from the 3D point p to the 2D image location p' , inherently present in a textured 3D model. We just leverage this information for augmenting 2D feature descriptors to 3D points. Also, since Barycentric coordinates are unique for a point lying inside the triangle, $(\lambda_1, \lambda_2, \lambda_3)$ are the barycentric coordinates of p' with respect to (t_1, t_2, t_3) as well, and the mapping between the 3D point p and 2d point p' is one-to-one, related by their barycentric coordinates in their respective faces. We use this inverse map $p' \mapsto p$ to assign features extracted in the texture-image I to the 3D points, thereby having a feature augmented model m . The algorithm is described in Algorithm 1.

3.2 Snapshot based Training

In this approach instead of relying on the texture map directly, we consider the real visual aspects of the model. This is similar to the traditional offline training stage performed on real objects with a key difference. Because of the availability of 3D models with us, we are free to choose virtual snapshot models of our choice and experiment with the outcome with respect to the quality of the model being generated.

Given a 3D model, we first take virtual snapshots from several directions based on a snapshot model. We then perform triangulation on the collection of features in the snapshots to get 3D points. The set of view dependent feature descriptors corresponding to a 3D point is clustered using Mean Shift clustering in the descriptor space and assigned to the 3D point,

thereby providing us a feature augmented 3D model. Because of the richness of our snapshot model, we only consider the points which are seen in atleast 5 different snapshots giving us a set of robust points in terms of visibility.

Snapshot Model. In order to take maximum advantage of the available 3D models, we intend to take snapshots from every direction to cover all viewing angles. This can be approximated by placing the model in the origin and pointing the camera towards the model from a set of uniformly discretized rotation angles. One of the way of achieving this is to use the faces (or vertices) a tessellated sphere built from a regular polyhedrons as viewpoint locations. Since the largest convex regular polyhedron is icosaheadron with 20 faces, we use a tessellated icosaheadron to approximate the sphere. The tessellation parameter controls how many times the triangles of the original icosaheadron are divided to approximate the sphere. Tesselation parameter of n would divide each triangle into four equilateral triangles recursively for n times. We generate feature augmented models with snapshots taken with tessellation level 0, 1 and 2 which gives a total of 20, 80 and 320 snapshots respectively as shown in Figure 2a. The trained models from all such sets are considered for evaluation.

In a snapshot, the 3d model is rendered in a white background with a directional headlight located at the center of the camera, and with other default rendering settings of Visualization Toolkit (VTK). One example of the reconstructed point cloud together with the position of the virtual cameras is shown in Figure 2b.

4 RECOGNITION FROM A SINGLE IMAGE

This is the online stage which involves object recognition in a calibrated query image I using a set of Trained 3D models $M = \{m_r\}, m_r = \{V_r\}$. The pres-

ence of 2D feature de-scriptors in our 3D model makes 6DOF recognition extremely easy. Here we briefly describe the two popular techniques we used for our evaluation for the shake of completeness.

PnP+RANSAC. This is the simplest and well studied form of object recognition. Features are extracted in a query image and matched against that in our trained models to get a set of 3D to 2D correspondences. These 3D - 2D point correspondences are used to compute the pose by one of the dedicated Perspective-n-Point problem (PnP) methods [Dementhon and Davis, 1995, Lepetit et al., 2009]. The PnP procedure is carried under the RANSAC scheme. Object is said to be recognized, if PnP converges with an error under a threshold in a fixed number of RANSAC iterations.

MOPED. Our main online recognition stage is built upon MOPED [Collet Romea et al., 2011], one of the most robust framework for object recognition. Following 7 steps are performed in sequence: *Feature extraction, Feature matching, Feature clustering, Hypothesis generation, Cluster clustering, Pose refinement and Pose recombination*. The notable addition of MOPED framework is the clustering of the features in the image space (for removing matching outliers) and clustering of the object hypothesis in a common coordinate space (for handling multiple instances). Readers are referred to the original paper for more details.

5 SIMULTANEOUS CAMERA CALIBRATION

When the camera parameters of the query image is not known we use the 3D - 2D correspondences to perform camera calibration instead of solving for PnP. As a result, for uncalibrated images, our trained model can be directly used as a standard marker for performing calibration. Because of the presence of large number of outliers, the calibration procedure needs to be performed under RANSAC with a large number of iterations. This is not a concern here as we consider a single known model instead of a big database. We described the procedure used in the following paragraphs.

Initialization. We assume a simple linear projection model in the first step for calibration. In this model, a 3D point X_i and its projection 2D point x_i is related by,

$$\lambda_i x_i = P X_i, \quad (1)$$

where $P = K[R \ t]$, K is the intrinsic matrix and $[R \ t]$ is the extrinsic matrix with R as a 3×3 rotation

matrix and t as a 3×1 vector denoting the translation. Our aim here is to find the parameters P and hence K, R, t from a given set of $X_i \leftrightarrow x_i$ correspondences.

System of equations of the form 1 for unknown P and λ_i is well studied and can be solved by the algorithm DLT. To find the matrix K and R , we do a RQ decomposition of first 3×3 submatrix of P .

Maximum Likelihood Estimation. To incorporate distortion along with the projection and to overall refine our intrinsics obtained in the section above, we find maximum likelihood estimate of the parameters by minimizing the function:

$$\sum_i \|x_i - \mathcal{P}_{K,R,t,D}(X_i)\|^2 \quad (2)$$

where K , R and t are the intrinsics, rotation and translation respectively as defined above, and $D = \{k1, k2, k3, k4\}$ is the set of non-linear distortion coefficients. $\mathcal{P}(X_i)$ is the projection of X_i including the non-linear distortion with the above parameters. This is a nonlinear minimization problem, which is solved with the Levenberg-Marquardt (LM) Algorithm. As an initial guess of the LM algorithm, we take $D = 0$, and K , R and t as obtained in the initialization step.

6 EVALUATIONS

6.1 Experimental Settings

Model Acquisition. We acquired 3D models using a light weight 3D scanner of 3Digify [3Digify, 2015] consisting of two household cameras and a projector. This scanner acquires the 3D geometry by projecting a fringe pattern and captures the distortion of this pattern over the object surface with two cameras. In the end we acquired high resolution textured 3D models of 7 different real objects of different types; namely **Lion**, **Totem**, **Energy-drink**, **Matriochka**, **Milk-carton**, **Whitener** and **Russian-cup**. Out of these, Milk-carton has dominant planar surfaces with synthetic texture and resembles planar models and surfaces with synthetic textures. Lion and Totem on the other hand have very complex shape with natural texture. Energy-drink and Whitener resembles synthetically textured cylindrical household models. Matriochka and Russian-cup form their own category with their partially oval shapes.

Methods. We used the SIFT-GPU [Wu, 2007] as our main feature extraction algorithm. In our snapshot based training, we used the default rendering parameters of Visualisation Toolkit (VTK) for taking virtual snapshots and subsequently, VisualSfM toolkit which

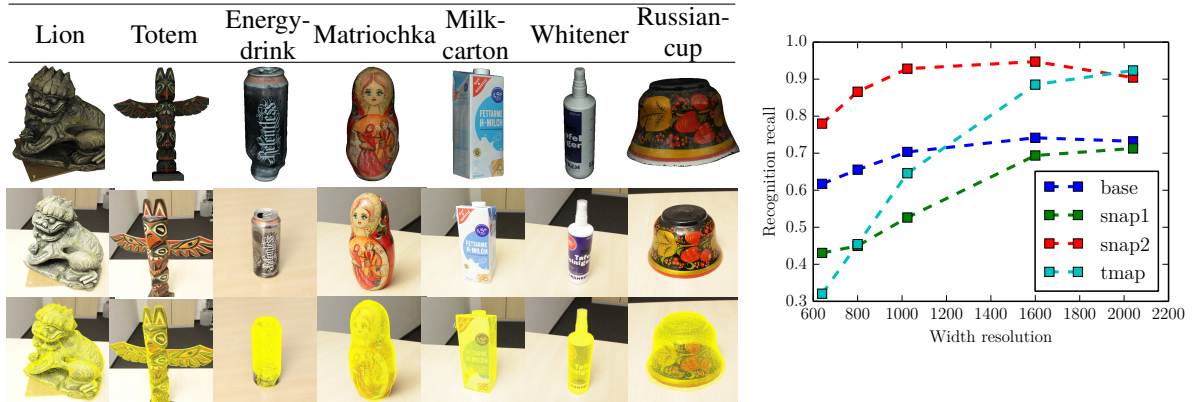


Figure 3: (**Left**) Models that are considered for evaluations. The first row shows the 7 acquired CAD models. The second row shows the images of the real objects of the corresponding models. The third row shows result of 6DOF recognition where mesh from the CAD models are reprojected on to the 2D images using the extrinsics found. Note that the images are zoomed towards the model for better visualization. (**Right**) Comparison of recognition recall of our methods with the existing **base** whose trained model is obtained by the manual way of taking pictures, segmenting and performing SFM.

Table 1: (**Left**) Comparison of object recognition recall with **MOPED** of our trained model. ‘All Resolution’ includes the results from the width-resolution 640, 800, 1024, 1600 and 2040 pixels. We achieved best results in our two highest resolutions (of width 1600 and 2040) which are shown separately under ‘Largest Resolutions’. (**Right**) Object recognition recall using **PNP+RANSAC** with images of width-resolution 1600 and 2040.

Models	All Resolutions			Largest Resolutions		
	snap1	snap2	tmap	snap1	snap2	tmap
Milk-carton	0.79	0.88	0.71	0.93	1.00	0.95
Totem	0.44	0.83	0.21	0.40	0.73	0.31
Lion	0.56	0.89	0.63	0.72	0.93	0.90
Whitener	0.34	0.48	0.63	0.57	0.82	0.80
Russian-cup	0.45	0.42	0.45	0.95	0.91	1.00
Energy-drink	0.57	0.52	0.54	0.93	0.79	0.88
Matriochka	0.63	0.58	0.62	1.00	1.00	1.00
Average	0.55	0.79	0.57	0.73	0.89	0.84

Models	snap1	snap2	tmap
Milk-carton	0.93	0.83	0.55
Totem	0.32	0.82	0.24
Lion	0.71	0.83	0.72
Whitener	0.15	0.15	0.15
Russian-cup	0.41	0.32	0.36
Energy-drink	0.67	0.76	0.59
Matriochka	0.82	0.84	0.61
Average	0.64	0.77	0.59

uses Multicore Bundle Adjustment [Wu et al., 2011], as our triangulation tool.

For each of the 7 3D models, we obtained the feature augmented models from texture-map based method (Section 3.1) which we call **tmap**, and snapshots based method (Section 3.2) with virtual snapshots taken with a tessellation level of 1 and 2, and call them **snap1**, **snap2** respectively.

Query Image Dataset. We captured more than 100 images for each of the 7 objects keeping them at various distance from the camera varying from 30 cms to 100 cms. Out of them we generated images of different resolutions width of 640, 800, 1024, 1600 and 2040 pixels (keeping the aspect ratio same). Therefore, each object in our object database is associated with more than 500 images with the total of more than 3500 images for the entire dataset.

6.2 Evaluation of Trained Models for Recognition

In this set of experiments we evaluate our trained models in terms of their ability to be recognized by an online recognition stage as discussed in Section 4. Because of its robustness, we chose the recognition method based on **MOPED** to compare the results of the different variation of our algorithm, namely **snap1**, **snap2** and **tmap**.

We use the Quality Score (Q-Score) defined in [Collet Romea et al., 2011] to consider an object to be recognized in its corresponding image. Q-Score is a correspondence-number independent score of a recognition hypothesis based on Cauchy distribution with a lower bound 0 and upper bound as the number of correspondences. In our case an object is considered to be recognized in its associated captured image when MOPED converges to a Q-Score of 5.

The comparison of our different methods can be

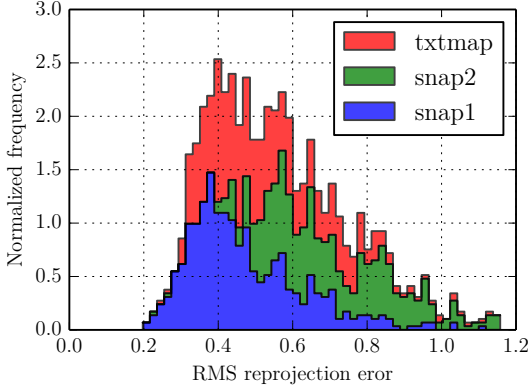


Figure 4: RMS reprojection error (pixels) from our calibration technique using the trained model. The histograms are *stacked* over each other for better visualization. Best viewed in color.

found in Table 1 (Left). As expected the highest recognition recall is found with **snap2** which considers 320 virtual snapshots. The second overall recognition recall is achieved by our very simple texture-map based method **tmap** and outperforms **snap1** which considers 80 virtual snapshots.

Comparison with the Baseline. In this experiment we compare our methods with the traditional manual way of creating feature augmented models from real objects. For this purpose we use our most complexly shaped object - Lion for evaluation. The baseline feature-augmented model (**base**) of Lion is created by manually taking 50 high quality images from different directions. Each of the images is then segmented for the object by manually creating a mask around the object in the image to remove background scene. These segmented images are then used for reconstruction to obtain sparse 3D point cloud with 3D points augmented with the clustered view dependent feature descriptors. The result of the final evaluation is shown in Figure 3 (Right). Our **snap2** comes out superior in all resolutions here as well. In higher resolution images our method **tmap** performs better than the **base**. This is because the scale of the query images matches to the scale of the texture map at the larger resolution.

Online Algorithm Independence. To show that our trained model is independent of the online stage, we perform and compare the results from a simple **PNP+RANSAC** (Section 4) based online recognition stage and compared with that of **MOPED**. Here we chose a RANSAC scheme with 500 iteration, 80% confidence and reprojection error threshold as 2 pixels. Objects are said to be recognized when the RANSAC converges with the above settings. The

Table 2: Comparison of calibration result of [Bouguet, 2008] and our method using the augmented model of **Lion+snap2** and images of size 2040x1360. ‘sample’ is the calibration results of one particular image; ‘mean’ and ‘deviation’ are the respective statistical functions on the calibration results over all the images.

params	Bouguet	sample	mean	deviation
fx	1364.00	1360.76	1368.83	68.54
1368.31	1364.41	1368.49	67.50	
cx	999.34	1005.48	1039.27	78.64
cy	690.20	715.21	663.81	50.99
rms	0.62	0.51	0.58	0.10

Table 3: Average RMS reprojection error of our different models.

	sna1	snap2	tmap
avg RMS (pixels)	0.47	0.69	0.53

results of the recognition recall with the images of width-resolution 1600 and 2040 are shown in Table 1 (Right). Because of no outlier detection a-priori of RANSAC we get comparably low recognition recall compared to MOPED. But an average of recognition recall of more than 50% on a simple PNP+RANSAC based recognition verifies that our trained model is independent of the online recognition algorithm.

6.3 Evaluation of Trained Models for Calibration

In this set of experiments we evaluate our trained models in terms of their ability to be used as a calibration rig. We used the object **Lion** for this purpose because of its highly complex shape which emphasizes the fact that our technique is different than most of the popular available calibration technique which depends on the planer nature of the calibration rig [Bouguet, 2008, Heikkila and Silven, 1997, Zhang, 1999]. As the model is fixed and known, we chose a large RANSAC iteration of 1000 and an RMS error threshold of 2 pixels in all our experiments for calibration.

Variation and Stability. Around 50 images of Lion were taken from random direction with a fixed focus camera. Without changing the focus and other settings of the same camera, 15 images of standard chessboard were taken as well. The images of the chessboard were then used for calibration using the popular Bouguet’s Camera Calibration Toolbox [Bouguet, 2008] for comparison. Because of its higher detection rate in PNP+RANSAC scheme we considered the the trained model **snap2** for performing calibration on the images of **Lion** for an extensive evaluation of variation of the intrinsics (Equation

1). Each image of Lion was calibrated separately using our simple DLT+MLE method (Section 5) under RANSAC. The mean and the standard deviation of the calibration results of all the images are compared and provided in Table 2. It is observed that, the RMS reprojection error of our technique is smaller than that of [Bouguet, 2008] in most of the cases. Because we only take one image for calibration, our result is tightly coupled with that particular image which is reflected with the low RMS error and moderate standard deviation over all the images.

RMS Error Analysis. In the next experiment we make an analysis over the RMS reprojection error over images of various types, sizes and focal lengths for all our modelling methods. For each model **snap1**, **snap2** and **tmap**, we calibrated all the images of **Lion** from ‘query image dataset’ (more than 500 images with width-resolution 640, 800, 1024, 1600 and 2040 pixels) and collected their RMS error. The distribution of RMS error is represented as histogram in Figure 4 and the mean RMS error is provided in Table 3. As shown, though the error from our method is spreaded over a good spectrum because of the various types of images used, our mean RMS error is small which makes our method a quick and reliable tool for camera calibration where an extreme accuracy is not a concern.

7 CONCLUSION

We have presented methods for creating feature-augmented models from CAD models for the purpose of 6DOF object recognition and camera calibration. The fully automatic procedure produces models that are capable of being recognized in single image with high accuracy with different flavours of online stage, and as a natural marker for the purpose of camera calibration.

In the future we look forward to consider view dependent global features (Eg. 2D shape context) to be computed on our virtual snapshots in an attempt to match them in query images. In this way we plan to include geometric information along with the texture in our trained models.

ACKNOWLEDGEMENTS

This work was partially funded by the BMBF project DYNAMICS (01IW15003).

REFERENCES

- 3Digify (2015). 3digify, <http://3digify.com/>.
- Aldoma, A., Tombari, F., Rusu, R., and Vincze, M. (2012). Our-cvfh oriented, unique and repeatable clustered viewpoint feature histogram for object recognition and 6dof pose estimation. In Pinz, A., Pock, T., Bischof, H., and Leberl, F., editors, *Pattern Recognition*, volume 7476 of *Lecture Notes in Computer Science*, pages 113–122. Springer Berlin Heidelberg.
- Bouguet, J. Y. (2008). Camera calibration toolbox for Matlab, http://www.vision.caltech.edu/bouguetj/calib_doc/.
- Collet Romea, A., Martinez Torres, M., and Srinivasa, S. (2011). The moped framework: Object recognition and pose estimation for manipulation. *International Journal of Robotics Research*, 30(10):1284 – 1306.
- Collet Romea, A. and Srinivasa, S. (2010). Efficient multi-view object recognition and full pose estimation. In *2010 IEEE International Conference on Robotics and Automation (ICRA 2010)*.
- D'Apuzzo, N. (2006). Overview of 3d surface digitization technologies in europe. In *Electronic Imaging 2006*, pages 605605–605605. International Society for Optics and Photonics.
- Dementhon, D. and Davis, L. (1995). Model-based object pose in 25 lines of code. *International Journal of Computer Vision*, 15(1-2):123–141.
- Hao, Q., Cai, R., Li, Z., Zhang, L., Pang, Y., Wu, F., and Rui, Y. (2013). Efficient 2d-to-3d correspondence filtering for scalable 3d object recognition. In *Computer Vision and Pattern Recognition (CVPR), 2013 IEEE Conference on*, pages 899–906.
- Heikkila, J. and Silven, O. (1997). A four-step camera calibration procedure with implicit image correction. In *Computer Vision and Pattern Recognition, 1997. Proceedings., 1997 IEEE Computer Society Conference on*, pages 1106–1112.
- Irschara, A., Zach, C., Frahm, J.-M., and Bischof, H. (2009). From structure-from-motion point clouds to fast location recognition. In *Computer Vision and Pattern Recognition, 2009. CVPR 2009. IEEE Conference on*, pages 2599–2606.
- Lepetit, V., Moreno-Noguer, F., and Fua, P. (2009). Epnp: An accurate o(n) solution to the pnp problem. *Int. J. Comput. Vision*, 81(2):155–166.
- Lowe, D. (2004). Distinctive image features from scale-invariant keypoints. *International Journal of Computer Vision*, 60(2):91–110.
- Rusu, R., Bradski, G., Thibaux, R., and Hsu, J. (2010). Fast 3d recognition and pose using the viewpoint feature histogram. In *Intelligent Robots and Systems (IROS), 2010 IEEE/RSJ International Conference on*, pages 2155–2162.
- Skrypnyk, I. and Lowe, D. (2004). Scene modelling, recognition and tracking with invariant image features. In *Mixed and Augmented Reality, 2004. ISMAR 2004. Third IEEE and ACM International Symposium on*, pages 110–119.

- Tombari, F., Salti, S., and Di Stefano, L. (2010). Unique signatures of histograms for local surface description. In *Computer Vision–ECCV 2010*, pages 356–369. Springer.
- Wu, C. (2007). SiftGPU: A GPU implementation of scale invariant feature transform (SIFT). <http://cs.unc.edu/~ccwu/siftgpu>.
- Wu, C., Agarwal, S., Curless, B., and Seitz, S. (2011). Multicore bundle adjustment. In *Computer Vision and Pattern Recognition (CVPR), 2011 IEEE Conference on*, pages 3057–3064.
- Zhang, Z. (1999). Flexible camera calibration by viewing a plane from unknown orientations. In *Computer Vision, 1999. The Proceedings of the Seventh IEEE International Conference on*, volume 1, pages 666–673. IEEE.